ORIGINAL ARTICLE

lajss.org
Latin American Journal of Solids and Structures

www.lajss.org

# Data-driven intelligent detection model of railway vehicle wheels flat

**Xiang Su[a], Guangwei Zhao[b], Yuxin Sun[a], Nan Li[a]***

[a] School of Artificial Intelligence, Beijing Technology and Business University–BTBU, Beijing, China. Email: 2130062113@st.btbu.edu.cn, sunyuxin429@163.com, linan@th.btbu.edu.cn

[b] China Academy of Railway Sciences Corporation Limited–CARS, Beijing, China. Email: 3029424234@qq.com

* Corresponding author

https://doi.org/10.1590/1679-78257776

## Abstract

For solving a large amount of data processing and reducing the cost to improve detection accuracy, this paper proposes an intelligent detection model for railway vehicle wheels flat. We propose an automatic data processing algorithm for labeling large-scale data to maximize the benefits of each experiment data. To improve the generalization of the detection model to improve the accuracy, we combine the vehicle dynamics simulation data and the simulation experiment data based on the single wheel rolling test bench to construct the data set for detecting the wheel flat. Different from the existing detection models, this paper provides a method for constructing the data sets, which is used to assist machine learning in constructing the intelligent detection model. The data set and its construction method can also promote the application of data mining in the field of railway transportation. This paper verified the effectiveness of the features obtained from data processing in the detection model. The data set is used to detect and identify the wheel flat and the recognition accuracy is 98.6%.

## Keywords

Wheel flat detection; vehicle dynamics; machine learning; feature extraction; axle box acceleration

## Graphical Abstract

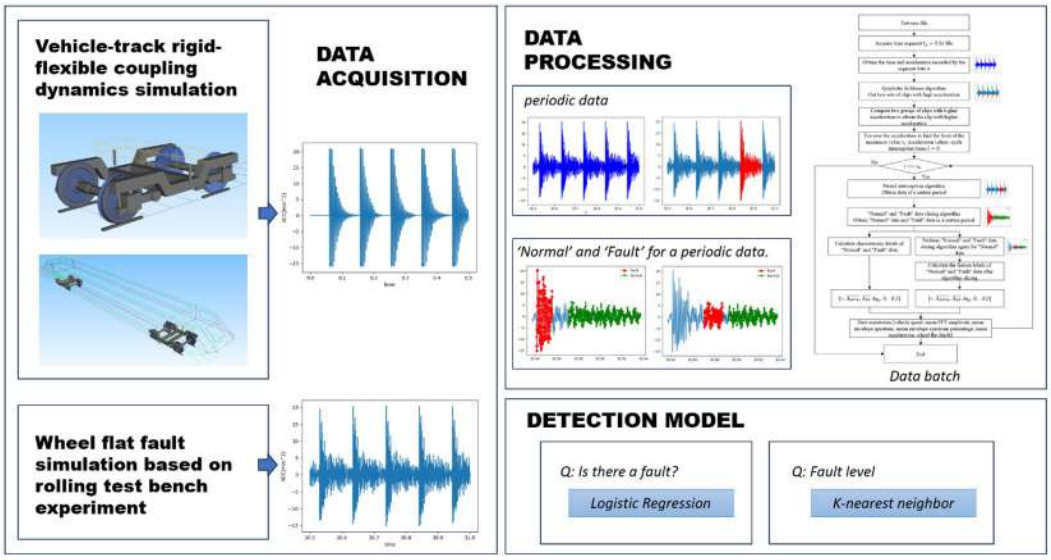


Received: July 22, 2023. In revised form: November 18, 2023. Accepted: December 18, 2023. Available online: January 10, 2024
https://doi.org/10.1590/1679-78257776

Latin American Journal of Solids and Structures. ISSN 1679-7825. Copyright © 2024. This is an Open Access article distributed under the terms of the Creative Commons Attribution License, which permits unrestricted use, distribution, and reproduction in any medium, provided the original work is properly cited.

## 1 INTRODUCTION

With the development of the economy, residents travel more frequently, and the speed of railway transportation has increased several times, which puts forward higher requirements for the safety and stability of railway transportation. As an important running part of a high-speed train, the wheelset always affects the safety of the train. It not only bears the full weight of the train and itself but also acts as a transmitter of force between the wheels and rails. However, when the train brakes, due to the improper operation of the driver, the braking system is not good enough, the wheel-rail adhesion force is reduced, and other factors, the braking force will be so large that the wheels are locked, which causes the abnormal friction between the wheel tread and the track will make some abrasion on the wheel tread (Xing, ZY et al. ,2022 and Bernal, E. et al. 2022). The wheel flat will bring huge additional impact force to wheel bearings and rails and periodically act on the wheel-rail system as the wheelset rotates. It is not only a factor that causes bearing and foundation damage but also poor vehicle operation quality. Extremely serious safety accidents such as bearing fractures and subversion will occur in severe cases. Therefore, to ensure the normal operation of high-speed trains, it is necessary to regularly detect and maintain the wheel tread (Trilla, A. et al.2021).

The current research on the detection methods of wheel tread flat is divided into two categories, which are static detection and dynamic detection (Liu XZ et al.,2018, Cao WJ et al.,2019 and Li CS et al.,2017a). The realization of static detection is to rely on the equipment to manually detect the state of the stationary wheel when the train stops. It has the advantages of convenient detection and maintenance and high detection accuracy, but it has the obvious disadvantages of a long time and low efficiency in detection. While the detection during train running is named dynamic detection. This method is convenient and efficient, and the detection accuracy is much higher than manual detection. The classical wheel flat dynamic detection technology includes the contact measurement method, electrical signal detection method, noise detection method, image detection method, ultrasonic detection method, vibration acceleration detection method, and axle box acceleration method.

The team of Beijing Jiaotong University (Gao, R et al.,2019) developed a system for measuring the wheel tread by using the parallelogram mechanism based on the measurement of the change value of the flange droop of the wheel, to realize the measurement of the abrasion and wear of the wheel flat. Although the measurement method is simple, easy for processing data, and has high measurement accuracy in the case of low train speed, the strong impact force generated by the wheel and rail will cause the measurement device damaged when the train is running at high speed. Therefore, this method is not suitable for the detection of wheel flats during high-speed train operation. The electrical signal detection method (Bernal E. et al.,2021) can be applied to the detection of high-speed trains. When the train is running at high speed, the wheel flat will lead to the formation of contact separation between the wheel and the track, so the length of the wheel flat is solved according to the separation time. Although this method can well reflect the length of the wheel flat, and the collected detection signal is not easy to be disturbed, it can not detect the wheel flat because the train and the track are not separated in low-speed operation, and the traffic order will be affected because the detection device needs to install an insulated track. The installation of detection equipment based on the noise measurement method (Komorski, P. et al.,2021) is simple. It determines the length and location of the wheel flat by collecting the sound signal of the impact between the wheel and the rail. However, the signal acquisition will be disturbed by the adjacent wheels, so the detection accuracy is poor and it can not meet the requirements of detecting wheel flat. To improve the detection accuracy and with the development of image processing technology (Zhou QB et al.,2019 and Xu JY et al.,2015) and photography technology, the image detection method has made some research. It is a high-definition shooting of the passing train wheel through the detection device and then completes the detection of the wheel flat based on machine vision (BERNAL, E J. et al.,2016). Although this detection method has high detection accuracy, the detection cost is too high and the installation is difficult. The ultrasonic detection method (Alireza Alemi. et al.,2017) is to install electromagnetic ultrasonic on the rail, and obtain defect-related information by analyzing the reflected ultrasonic surface wave. Although the ultrasonic detection method is accurate, the economic benefit of the measuring equipment is not high. The principle of the vibration acceleration detection method is to analyze the vibration information of the track to obtain the wheel tread defect information by installing acceleration and wheel weight sensors under the rail. Although this detection method can adapt to the high and low-speed operation of the train, it is difficult to avoid the interference of adjacent wheels on the collected signal.

Based on the above detection methods, these all need to install measurement devices on the track, and the detection can only be completed when passing the track. The problem is that most of the measurements are only suitable for low-speed operation and are not practical on the actual running train, and there are problems such as high detection cost and susceptibility to interference from adjacent wheelsets.

Therefore, it is necessary to solve high-speed train detection and improve detection efficiency. We proposed a detection method based on axle box acceleration. If the detection device is installed on the train, the wheel can be continuously monitored by obtaining the train state, which can effectively eliminate the interference of adjacent wheelsets and can more directly measure the vibration signal caused by wheel flat. The axle box acceleration method is based on this idea. Its realization principle is to install the acceleration on the axle box and to complete the detection of the wheel flat by analyzing the obtained acceleration signal. Due to the complexity of the collected vibration signal, the vibration signal contains information not only on the wheel tread but also on the track (Xiao Q. et al.,2021). Therefore, extracting the wheel flat feature from the vibration signal is the key to detecting the damage. Based on the idea of reverse engineering, Yi et al.(2022) used the axle box vibration acceleration signal to infer the running state of the wheelset and proposed a new resonant excitation loading method. The amplitude of the frequency of the axle box resonance characteristic is used to characterize the axle box vibration response signal to infer the wheel running state, which provides a basis for quantitative evaluation of the local damage of the wheel. Li YF et al. (2017) discussed the ability of morphological analysis in railway vehicle plane fault detection and proposed an adaptive multi-scale morphological filtering algorithm. The algorithm was used to diagnose and evaluate the dynamic response of the axle box calculated by the constructed vehicle dynamics model and the wheel plane model, and the real-time diagnosis of wheel plane fault was realized. By constructing a dynamics model of a vehicle-track rigid-flexible coupling system, Song et al. (2021) studied the quantitative relationship between axle box acceleration and wheel flat of high-speed trains in the time domain and frequency domain. They used the improved empirical mode decomposition and Wigner-Ville distribution time-frequency domain method to analyze the axle box acceleration calculated by simulation. It is proved that the axle box acceleration can not only detect the wheel flat but also identify the damage degree.

Although the detection method based on the axle box acceleration can realize the real-time monitoring of the running state of the vehicle wheel, and the detection accuracy is high, there are problems such as multiple data acquisition channels, the large amount of data processing, and the high cost of detection (Mohammadi M. et al.,2023). Therefore, how to intelligently solve the processing of a large amount of data, reduce the detection cost and improve the accuracy of damage identification are the main problems.

To solve the above problems, this paper, combined with the machine learning model, from the perspective of accumulating and perfecting the detection data to maximize the benefit of each experiment, proposes an automatic whole-process algorithm for labeling the experimental detection data set to solve a large amount of data processing. Based on the idea of data fusion, we compare and evaluate the accuracy between simulation and real-world response based on the detection model to verify the reliability of data fusion. To improve the accuracy generalization ability of the detection model under the premise of saving experimental economic costs, this paper finished integrating the vehicle dynamics simulation data and real experimental simulation data based on the idea of data fusion and constructed the wheel flat detection model. The contributions are as follows:

1. Vehicle dynamics simulation and rolling test bench experiment: the fault signal of the wheel flat is obtained by simulating the installation of an acceleration sensor on the axle box based on SIMPACK and ANSYS combined vehicle dynamics simulation and rolling test bench experiment simulation.
2. An automatic whole-process algorithm for labeling the experimental detection data set: the slicing and feature extraction of the fault signal is realized based on quadratic K-Means, and using the mixed analysis features of the time domain and frequency domain to label and then generate in batch to construct the data set.
3. Data-driven intelligent detection model: Firstly, construct the detection model for different classification problems. Secondly, find the optimal detection model by analyzing and discussing the detection accuracy of the detection model constructed by combining logistic regression and K-nearest neighbor in the time domain, frequency domain, and time-frequency domain respectively. Finally, verify the influence of data fusion on the detection model.

The second section describes the data acquisition method and the fusion of multi-source data. By establishing the vehicle-track coupling dynamics simulation model and the rolling test bench experiment, we obtained the axle box acceleration under different speeds and different wheel flat damage and then verified the reliability and the similarity between the simulation data and the experiment data. Section 3 proposed an automatic whole-process algorithm for labeling the experimental detection data set for the experimental data obtained in Section 2, and created a data set for training detection models. Section 4 describes the process of constructing an intelligent detection model for wheel flat, we found the optimal model by analyzing the accuracy of wheel flat detection combined with different machine learning models and different labeling features, and verified that the detection model trained with data fusion has better performance. Section 5 summarizes the conclusions and innovations, and puts forward suggestions for future work. The contribution and writing ideas of this paper are shown in Figure 1.

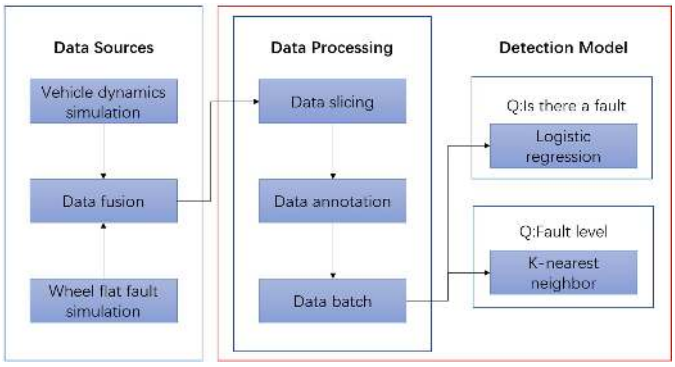


**Figure 1** The contribution and writing ideas.

## 2 DATA ACQUISITION

Railway transportation is closely related to passenger safety and it is not allowed to drive faulty trains on the railway, so it is difficult to obtain data through real experiments. Simulation research is mostly applied to the research problem of detecting faulty train running. Although the cost of the simulation experiment is low, the problem with the simulation experiment is that the result is too ideal, while the real experimental data contains a lot of noise. To make up for this problem, the data obtained from the real experiment based on the rolling test bench can characterize the actual running state of the faulty train running to a certain extent. Considering that there is a certain error between the experimental data based on the rolling test bench and the data measured by the real railway driving fault train, as mentioned above, driving the fault train is not allowed. Due to the similarity between the Simpack dynamic simulation and the test bench data under the same operating conditions of the vehicle (Section 2.1 and Section 2.2), we thought that the 1: 1 single-wheel rolling experiment based on the lab can replace the real vehicle running state. However, the real experiment based on the rolling test bench has the following two problems. Firstly, the experiment materials cannot be used repeatedly which leads to a high cost for completing the experiment; Secondly, the data of train axle box acceleration with different running speeds and different wheel flat obtained are less, so the generalization of training samples provided for subsequent training using machine learning model is poor.

In this paper, we obtained the simulation data building the rigid-flexible coupling dynamic model simulation of vehicle track based on SIMPACK combined with ANSYS and the experiment data doing the real experiment based on 1: 1 single wheel rolling test bench. Not only does the experiment result from obtain with the rolling test bench make up for the ideal simulation result, but also the rigid-flexible coupling dynamic model simulation of vehicle track based on SIMPACK combined with ANSYS reduces the high cost of a real experiment, and solves the problem that the test data of train axle box acceleration with different fault conditions is less.

### 2.1 Vehicle-track rigid-flexible coupling dynamics simulation

#### 2.1.1 Wheel flat model

We reproduced the modeling method of the wheel flat mentioned by the Jaeseok Shim's team (Shim et al., 2022). In the SIMPACK creation wheelset module, we built the wheel model with the wheel flat by defining the function of the radius deviation. The model description of the wheel is shown in Figure 2. Since the wheel radius R and the flat length L is known, we can calculate the angle α corresponding to the flat length and then calculate the A and B coordinates from the angle α (see Formulas 1-3).

$$\theta = \arccos\frac{L}{2R} \tag{1}$$

$$h = \frac{L}{2}\tan\theta \tag{2}$$

$$\alpha = \arccos\frac{h}{R} \tag{3}$$

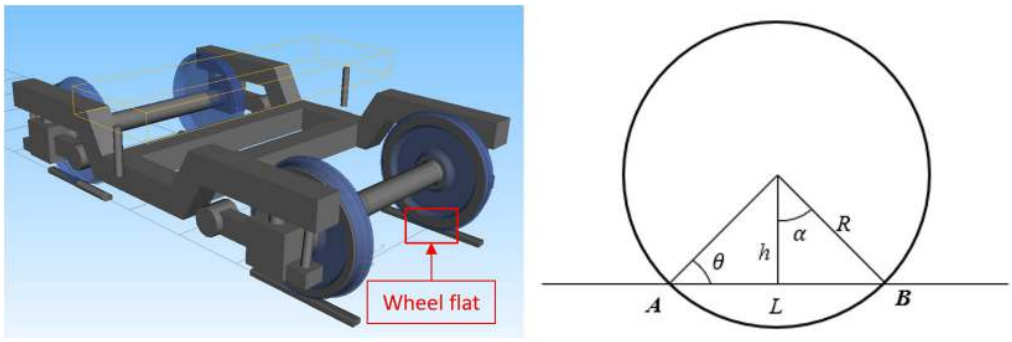


**Figure 2** The model description of the wheel with wheel flat.

Taking the angle α and radius R as input, we build the modeling of the wheel flat by editing the script of SIMPACK to define the function and confirm the model's correctness by detecting the Z-direction distance between the wheel and the track. (See Figure 3).

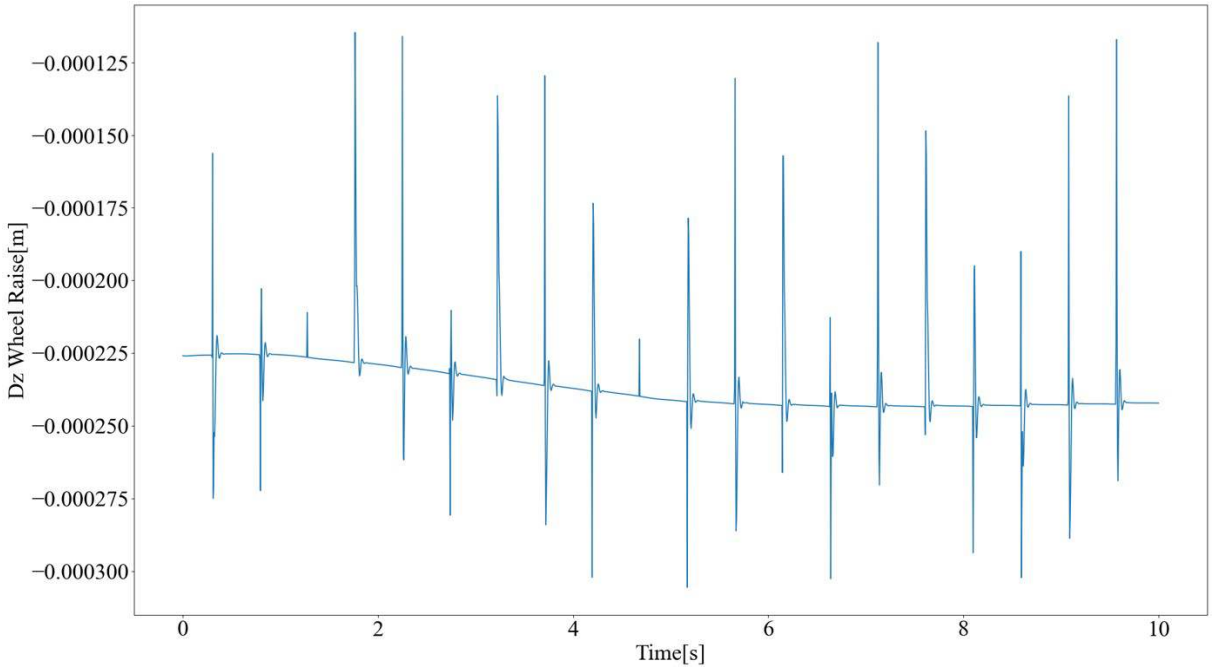


***Figure 3*** *The Z-direction wheel raises with the train's running speed of* $20km/h$ *. The sampling frequency is 100Hz.*

2.1.2 Vehicle dynamics simulation

To better obtain the experimental results of the axle box acceleration at different running speeds of the train running, it is necessary to establish a flexible wheelset to replace the rigid wheel set in SIMPACK, and then edit the script to add the definition of the wheel flat described function.

(1) Establish a flexible wheelset

The reason why we built the flexible wheelset model of the wheelset is to consider the influence and response of the flexible body in the dynamic model. Therefore, to build the rigid-flexible coupling dynamics model, we completed importing the wheelset, completing the geometric cleaning, meshing, grid quality inspection, and assigning material properties to the model in HYPERMESH and imported the HYPERMESH export results into ANSYS to complete the generation and modal calculation of the substructure.

To improve the calculation performance of ANSYS, we need to reduce the wheelset foundation model to a substructure model. We selected the first 10 modal differences and considered it reasonable to be within 5 % to verify the rationality of the substructure model. The comparison results are shown in Table 1.

**Table 1** Modal quality inspection of substructure model.

| Order number | Modal analysis of basic model | Modal analysis of substructure model | Error |
|---|---|---|---|
| 1 | 87.684 | 87.684 | 0.00% |
| 2 | 102.3 | 102.33 | 0.029% |
| 3 | 102.3 | 102.33 | 0.029% |
| 4 | 184.16 | 184.33 | 0.092% |
| 5 | 184.16 | 184.33 | 0.092% |
| 6 | 324.72 | 325.45 | 0.22% |
| 7 | 328.79 | 330.28 | 0.305% |
| 8 | 328.79 | 330.28 | 0.305% |
| 9 | 468.47 | 470.62 | 0.458% |
| 10 | 468.47 | 470.62 | 0.458% |

(2) Vehicle-track model

After completing the establishment of a flexible wheelset, we imported the wheelset flexible body into the vehicle-track model in SIMPACK (see Figure 4-5). The vehicle model parameters in this paper reference a certain type of EMU. The vehicle model parameters in this paper reference a certain type of EMU. The relevant vehicle body, bogie, and track information and specifications are shown in Table 2-4.

**Table 2** Modelling values of length and mass

| Parameter | Unit | Value |
|---|---|---|
| Vehicle mass | $(\boldsymbol{ton})$ | 26.1 |
| Wheelbase | $(\boldsymbol{mm})$ | 2500 |
| Bogie mass | $(\boldsymbol{ton})$ | 2.6 |
| Wheelset mass | $(\boldsymbol{ton})$ | 2.1 |
| Axle box mass | $(\boldsymbol{ton})$ | 0.108 |

**Table 3** Modelling values of inertia and stiffness

| Parameter | Unit | Value |
|---|---|---|
| Body $\boldsymbol{I_{XX}}$ | $(\boldsymbol{kg \cdot m^2})$ | 84560 |
| Body $\boldsymbol{I_{YY}}$ | $(\boldsymbol{kg \cdot m^2})$ | 1278900 |
| Body $\boldsymbol{I_{ZZ}}$ | $(\boldsymbol{kg \cdot m^2})$ | 1102730 |
| Bogie $\boldsymbol{I_{XX}}$ | $(\boldsymbol{kg \cdot m^2})$ | 2106 |
| Bogie $\boldsymbol{I_{YY}}$ | $(\boldsymbol{kg \cdot m^2})$ | 1424 |
| Bogie $\boldsymbol{I_{ZZ}}$ | $(\boldsymbol{kg \cdot m^2})$ | 2600 |
| Wheelset $\boldsymbol{I_{XX}}$ | $(\boldsymbol{kg \cdot m^2})$ | 756 |
| Wheelset $\boldsymbol{I_{YY}}$ | $(\boldsymbol{kg \cdot m^2})$ | 84 |
| Wheelset $\boldsymbol{I_{ZZ}}$ | $(\boldsymbol{kg \cdot m^2})$ | 1029 |
| Primary longitudinal stiffness | $(\boldsymbol{MN/m})$ | 14.7 |
| Primary lateral stiffness | $(\boldsymbol{MN/m})$ | 1.5 |
| Primary vertical stiffness | $(\boldsymbol{MN/m})$ | 9800 |
| Secondary longitudinal stiffness | $(\boldsymbol{MN/m})$ | 0.15876 |
| Secondary lateral stiffness | $(\boldsymbol{MN/m})$ | 0.15876 |
| Secondary vertical stiffness | $(\boldsymbol{MN/m})$ | 0.18914 |

**Table 4** Modelling values of track information

| Parameter | Unit | Value |
|---|---|---|
| Gauge | $(\boldsymbol{mm})$ | 1435 |
| Railway type | - | UIC 60 rail |
| Wheel-rail contact type | - | Kalker Contact |
| Friction coefficient | - | 0.4 |

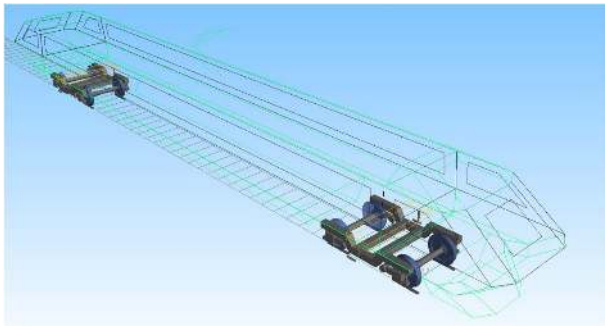

**Figure 4** Railway vehicle model.

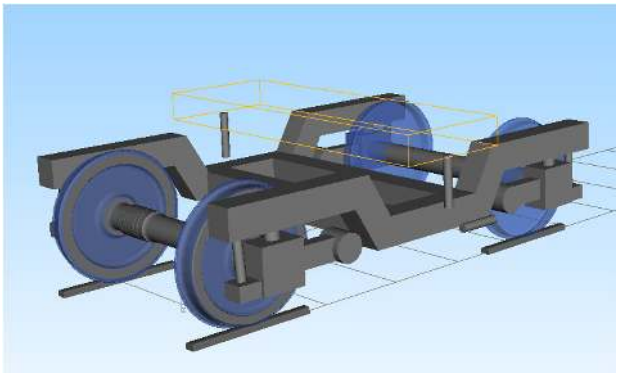

**Figure 5** Bogie model.

After establishing the vehicle model, we added an acceleration sensor on the axle box (See Figure 6) to measure the wheel flat signal. The measurement principle is to calculate the impact force between the wheel and the rail to infer the axle box acceleration in the X, Y, and Z directions generated under the impact force. The experimental results are shown in Figure 7.

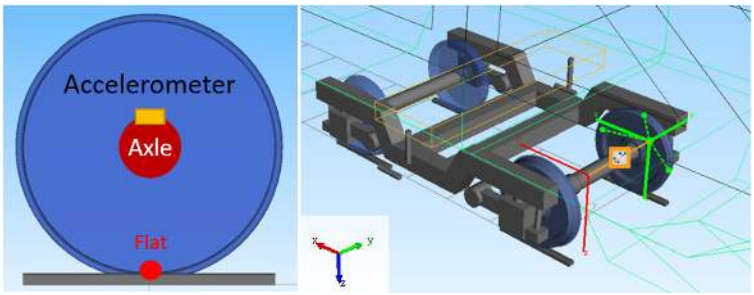


**Figure 6** The axle box acceleration measurement installation schematic in Simpack.

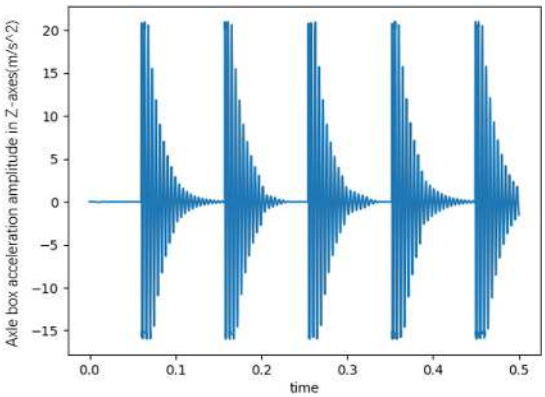


**Figure 7** Acceleration results of axle box with the vehicle speed of $100km/h$ and wheel flat depth of $0.2mm$. The sampling frequency is 1000Hz.

### 2.2 Wheel flat fault simulation based on rolling test bench experiment

To make up for the ideal simulation results, we completed the experiment of simulating the vehicle wheel flat fault based on the 1: 1 single wheelset rolling test bench which is mainly composed of a test bench, driving wheel (simulated rail), moving wheel pair, hydraulic loading device, frequency modulation driving motor and console.The simulation process of the experiment is rough as follows: a high-strength plastic belt is pasted around the wheel tread, and the actual wheel flat is simulated according to the thickness of the plastic belt and the gap of the plastic belt. The thickness of the plastic belt represents the depth of the wheel flat. and the result data is obtained by the installed axle box acceleration measurement sensor. The test results are shown in Figure 8, which are expressed as the axle box acceleration results of the simulated train running at a speed of $100km/h$ and a wheel flat depth of $0.2mm$.

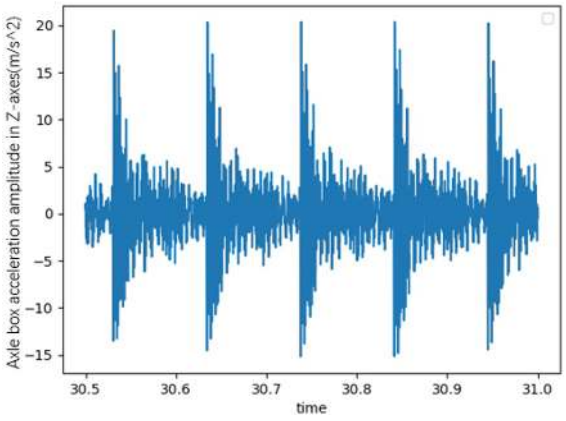


**Figure 8** Acceleration results of axle box with the vehicle speed of $100km/h$ and wheel flat depth of $0.2mm$. The sampling frequency is 1000Hz.

### 2.3 Data fusion

This paper aims to solve the problem that the experimental cost is high and the amount of simulation test data is small, which is not enough to realize the data-driven construction of the vehicle wheel flat detection model. We integrated data obtained from vehicle dynamics simulation and wheel flats fault simulation based on the rolling test bench experiment, and then construct the data-driven wheel flat detection model. Therefore, we verified the reliability of the fusion of simulation results and the real experimental results. Firstly, based on artificial vision, we can compare the axle box acceleration data obtained from vehicle dynamics simulation and wheel flats fault simulation based on the rolling test bench experiment. The results show that the trend and numerical range periodically characterizing wheel flat of axle box acceleration is similar (see Figure 6 and Figure 7). Secondly, to quantify the rationality of the data, we completed creating the training set by using the data processing method described in section 3. The detection model (the binary classification detection model) constructed in section 4 is used to detect the existence of the wheel flat, and the accuracy rate of the model is 90.24 %. The results show that only the data measured in the real world is used for training, when the model encounters the ideal simulation results, the robustness of the detection model is not strong. and the accuracy rate of more than 90 % indicates that the simulation data and the real-world measured data are correlated, and the fusion of simulation data and real data is reliable. The reliability verification of simulation data is shown in Table 5.

**Table 5** Reliability verification of the fusion of simulation and data.

| Attributes | Value | Description |
|---|---|---|
| Number of training set samples | 68 | Based on the 1: 1 single wheelset rolling test bench in the lab, the real experimental data of the vehicle at different running speeds are obtained by manually grinding the wheel flat with a depth of 0.2 mm on the wheel. |
| Number of test set samples | 41 | The SIMPACK simulation experiment data of axle box acceleration with wheel flat depth of 0.2mm and train running at different speeds |
| Machine learning model | - | Logistic regression |
| Precision ratio | 90.9% | - |
| Mean-square error (MSE) | 0.0975 | The smaller the MSE value is, the more accurate the model is. |
| R-square | 0.609 | Through the change of data to characterize the quality of a fit, the value is closer to 1, which shows that the model fits the data better. |

Therefore, the simulation results obtained from the vehicle-track rigid-flexible coupling dynamic model can be used as the input for training the intelligent wheel flat detection model, which provides support for improving the model generalization ability.

## 3 DATA PROCESSING

### 3.1 Data fusion

For the data of $d = 0.2mm$ and $v = 100km/h$, we analyze the envelope spectrum of a cycle of fault data and normal data respectively (Fault data with wheel flat, which calls it 'Fault' data, while normal data without wheel flat, which calls it 'Normal' data). The amplitude change of the envelope spectrum of the fault data with wheel flat is more obvious than that of the normal data (see Figure 9).

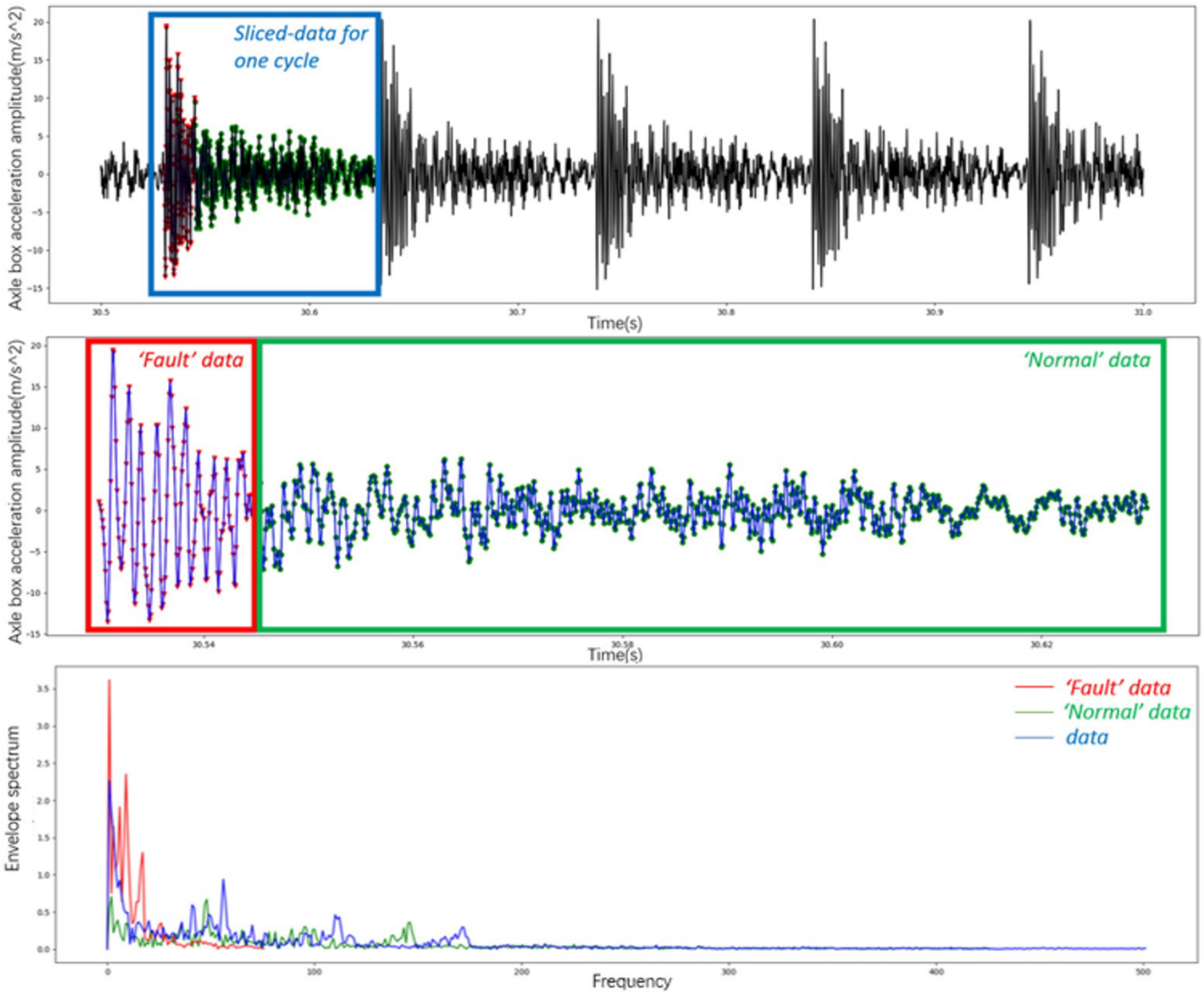


**Figure 9** Envelope spectrum analysis results of 'Fault' data and 'Normal' data.

To further obtain the signal characteristics of the wheel flat, we propose to automatically slice the experimental data. The 'Fault' and 'Normal' data are extracted from the sliced data of the vehicle wheel running for one week. Because manual data slicing is time-consuming and laborious, we propose an automatic data processing algorithm based on two-step of K-Means to complete the extraction of periodic fragment data and split it into 'Fault' data and 'Normal' data.

The algorithm steps are as follows:

Given the radius of the wheelset R and the vehicle speed v, the time T of the vehicle wheel running for one week is obtained (see Formulas 4):

$$T = \frac{2\pi R}{v} \tag{4}$$

According to the experimental data time segment $t_p$, it can be obtained that the data contains the number of wheel revolutions $n_v$ (see Formulas 5):

$$\mathrm{n_v} = \frac{\mathrm{t_P}}{\mathrm{T}} \tag{5}$$

According to the sampling frequency $f$ of the data, the data number n of the vehicle wheel running for one week can be calculated $n_p$ (see Formulas 6):

$$n_p = \frac{t_p f}{n_v} \tag{6}$$

The experimental data is shown in Figure 10 (a). Firstly, obtain the acceleration of the experimental data and use K-Means once, the number of clusters is $k = 2$. The clustering results are shown in Figure 10 (b). The data is divided into two categories according to acceleration which is $a = 0$. Secondly, obtain the data of acceleration which is $a > 0$ part, and use K-Means again. The number of clusters is $k = 2$. The clustering results are shown in Figure 10 (c). The fault data with the wheel flat can be extracted. For the data of acceleration which is $a < 0$ part, perform the same steps. The fault data with the wheel flat is shown in Figure 10 (d).

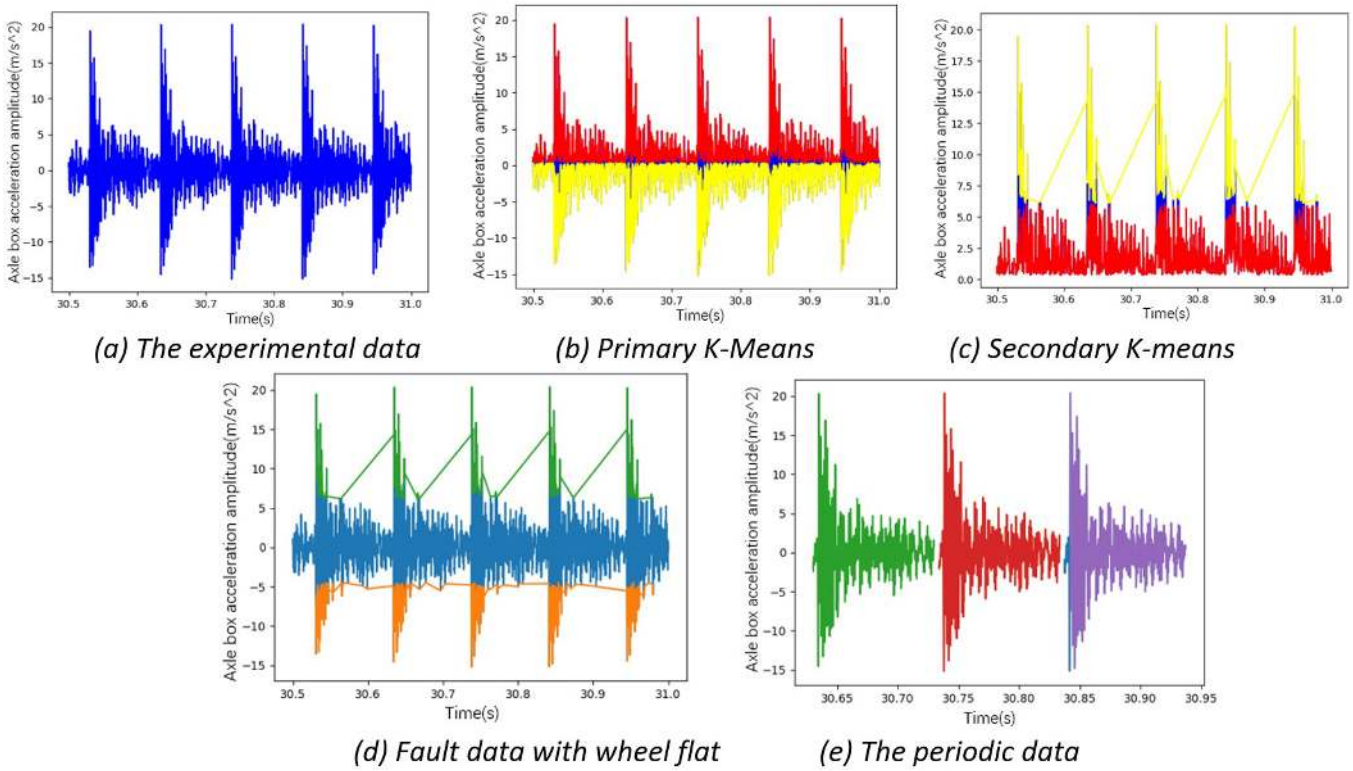


**Figure 10** The slicing process of obtaining periodic data.

Then, compare two groups of fault data and choose a set with higher acceleration. According to the turns number $n_v$ of wheel rotations we calculated, retrieve for a set with higher acceleration we choose to obtain the first $n_v$ acceleration values of the maximum value and its corresponding time index. Finally, intercept periodic data according to the data number $n_p$ of the vehicle wheel running for one week. The slice result is shown in Figure 10 (e).

For the intercepted periodic data fragment (see Figure 11 (a)), use two-step K-Means to obtain two sets of fault data with wheel flat as shown in Figure 11 (b), and then compare the two sets of data to obtain the value of the previous time as the starting point of the 'Fault' data.

For the determination of the slice endpoint, we compare the length of the fragments of the two sets of fault data and select the data with a more advanced time as the slice endpoint of the 'Fault' data. At the same time, to prevent the slice endpoint may contain normal data which will affect the envelope spectrum analysis to a certain extent, we compare whether the data length from the determined slice start point to the endpoint satisfies less than a quarter of the periodic data. If satisfied, intercept the 'Fault' data, while if not, we intercept the length of the 'Fault 'data to a quarter of the periodic data, that is, the slice endpoint index is the start point index plus a quarter number of the periodic data. Two-thirds of the data after the interception of the periodic data is used as normal data. It shows the slice results we obtained which are the fault data with the wheel flat and the normal data without the wheel flat (see Figure 11 (c)).

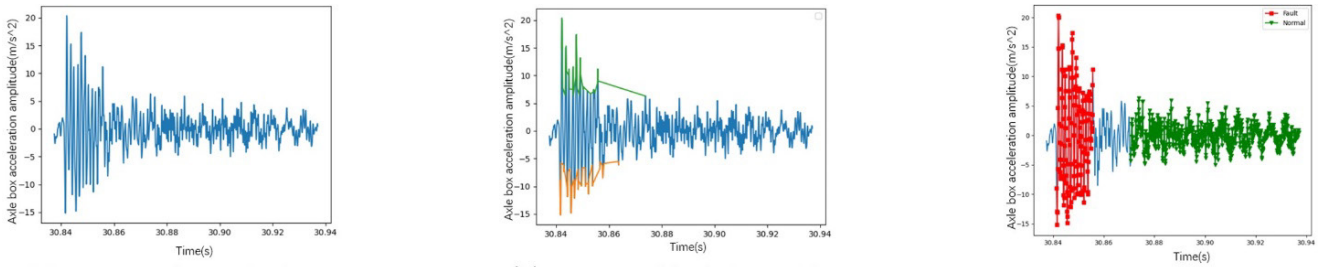


*(a) Intercepted periodic data* *(b) Two sets of fault data with wheel flat after two-step K-Means* *(c) 'Fault' and 'Normal' data*

**Figure 11** Data interception of 'Normal' and 'Fault' for a periodic data.

### 3.2 Data annotation

For the experimental record file with time segment $t_p = 0.5s$, completed to slice the periodic data slice described in Section 3.1 (see Figure 12 (a)), and then slice it to obtain the 'Normal' and 'Fault' data (see Figure 12 (b)). It is necessary to slice the 'Normal' data again with 'Normal' and 'Fault' data as a reference to make up for the lack of normal train running data, as shown in Figure 12 (c).

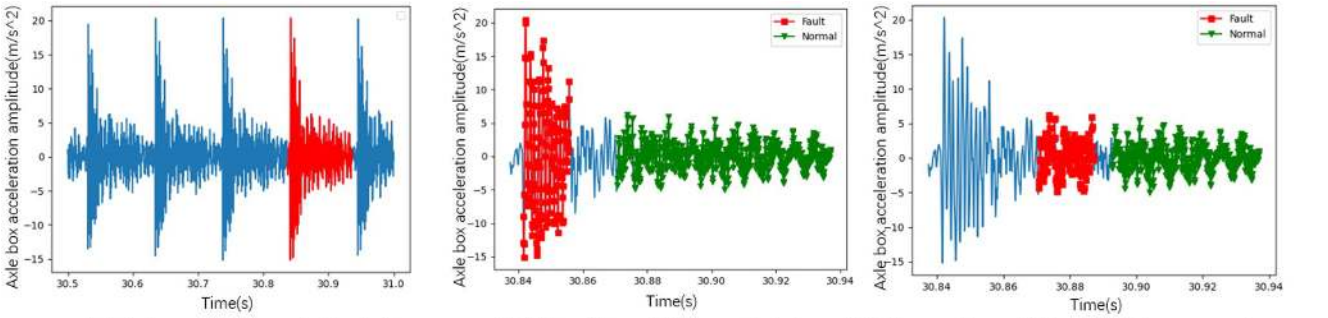


*(a) Intercepted periodic data.* *(b) 'Fault' and 'Normal' data.* *(c)'Normal' and 'Fault' data as a reference*

**Figure 12** Data preparation.

The data set label proposed in this paper includes vehicle speed, mean FFT amplitude, mean envelope spectrum, mean envelope spectrum percentage, mean acceleration, and wheel flat depth. The definition is as follows:

1. Vehicle speed $\boldsymbol{v}$

According to the fusion data file obtained from the experiment (see Table 6), the vehicle speed is different. Therefore, the vehicle speed is marked as different labels shown in the table.

**Table 6** Different vehicle speeds marked different labels

| Speed | Label |
|---|---|
| $\boldsymbol{v = 100km/h}$ | 100 |
| $\boldsymbol{v = 150km/h}$ | 150 |
| $\boldsymbol{v = 200km/h}$ | 200 |
| $\boldsymbol{v = 250km/h}$ | 250 |
| $\boldsymbol{v = 300km/h}$ | 300 |
| $\boldsymbol{v = 350km/h}$ | 350 |
| $\boldsymbol{v = 400km/h}$ | 400 |

2. Mean FFT amplitude $\overline{\boldsymbol{A_{FFT}}}$

FFT represents the Fourier transform. The purpose of the transform is to transform the signal in the time domain into the frequency domain. The mean FFT amplitude refers to calculating the mean value processing which is the data obtained after the fast Fourier transform of the slice signal. The mean FFT amplitude is recorded as $\overline{A_{FFT}}$ , The definition is as follows (see Formulas 7):

$$\overline{A_{FFT}} = \frac{\sum_{i=0}^{n} A_{FFTi}}{n} \tag{7}$$

Where, $A_{FFT}$ represents the amplitude at all frequencies after fast Fourier transform.

Therefore, the mean FFT amplitude of the 'Fault' data is: $\overline{A_{FFTF}} = \frac{\sum_{i=0}^{n} A_{FFTFi}}{n}$ , while 'Normal' data is: $\overline{A_{FFTN}} = \frac{\sum_{i=0}^{n} A_{FFTNi}}{n}$ .

3. Mean envelope spectrum $\overline{\boldsymbol{A_E}}$

The envelope spectrum refers to the data obtained by the FFT transform of the envelope signal which is enveloped for the extreme value obtained by the signal after Hilbert transform.

The mean envelope spectrum is the mean processing of all envelope spectrum amplitude $A$ obtained by the slice data.

The mean envelope spectrum is recorded as $\overline{A_E}$ , It is defined as follows (see Formulas 8):

$$\overline{A_E} = \frac{\sum_{i=0}^{n} A_i}{n} \tag{8}$$

Therefore, the mean envelope spectrum of the 'Fault' data is: $\overline{A_{EF}} = \frac{\sum_{i=0}^{n} A_{Fi}}{n}$ , while 'Normal' data is: $\overline{A_{EN}} = \frac{\sum_{i=0}^{n} A_{Ni}}{n}$ .

4. Mean envelope spectrum percentage $\boldsymbol{A_{\mathrm{Ep}}}$

The mean envelope spectrum percentage $A_{\mathrm{Ep}}$ proposed in this paper is extracted based on the envelope spectrum and the mean envelope spectrum. The mean envelope spectrum percentage $A_{\mathrm{Ep}}$ is defined as follows (see Formulas 9):

$$A_{\mathrm{Ep}} = \frac{\overline{A_{EF}} - \overline{A_{EN}}}{\overline{A_{EF}}} \tag{9}$$

Among them,

1) $\overline{A_{EF}}$ is the mean envelope spectrum of the 'Fault' data.

2) $\overline{A_{EN}}$ is he mean envelope spectrum of the 'Normal' data.

The mean envelope spectrum percentage is proposed by optimizing and improving the result of experimental data. First, after the envelope spectrum calculation of the slice signal, we choose the amplitude at a fixed frequency according to the frequency analysis. It is found that the characteristics cannot be distinguished by only labels considering different vehicle speeds and wheel flat depth. The result is shown in Figure 13. Since the vehicle speed is known, we can obtain the fixed frequency at $v = 100km/h$ 、 $v = 150km/h$ 、 $v = 200km/h$ 、 $v = 250km/h$ 、 $v = 300km/h$ 、 $v = 350km/h$ 、 $v = 400km/h$, and obtain the amplitude after envelope spectrum analysis with this fixed frequency. The experimental results show that the envelope spectrum amplitude at a fixed frequency cannot distinguish the depth of the wheel flat well. At the same time, the experimental fault simulation data lacks the acceleration data measured by the normal wheel running without the wheel flat, so it is impossible to give the reference to compare the envelope spectrum amplitude at the fixed frequency between the normal and fault train running.

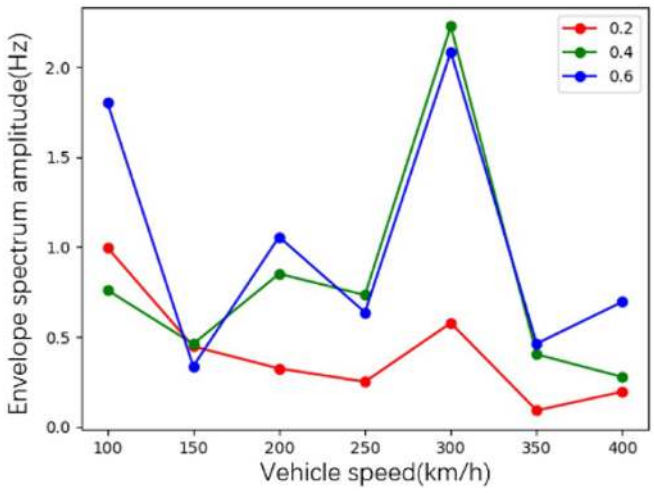


**Figure 13** The envelope spectrum amplitude at a fixed frequency under different vehicle speeds and wheel flat depth

Therefore, based on this exploration, we try to think about whether the mean of amplitude after envelope spectrum analysis can be used to characterize the wheel flat feature. As shown in Figure 14, the experiment shows that under different vehicle speeds, the mean value of the envelope spectrum for 'Normal' and 'Fault' data cannot well distinguish whether the vehicle has wheels flat.

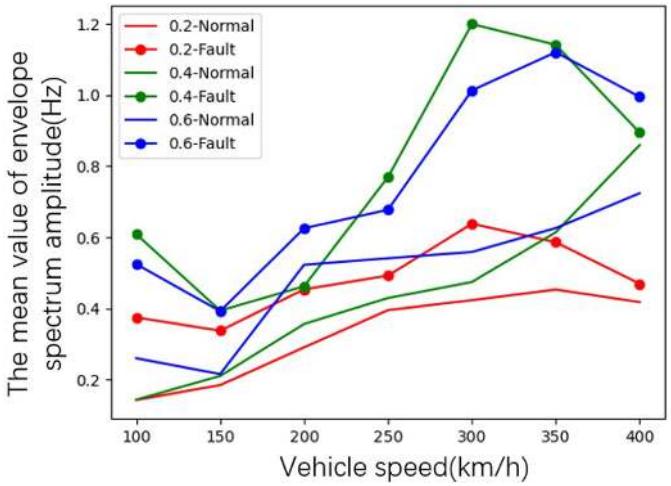


**Figure 14** The mean value of envelope spectrum amplitude under different vehicle speeds and wheel flat depth.

Based on these explorations, we try to use the mean envelope spectrum percentage to find the connection between 'Normal' and 'Fault' data to make up for the lack of acceleration data measured by the experimental fault simulation which is these data obtained from the normal vehicle operation without wheel flat. As shown in Figure 15, the mean envelope spectrum percentage can clearly distinguish whether the wheel flat exists.

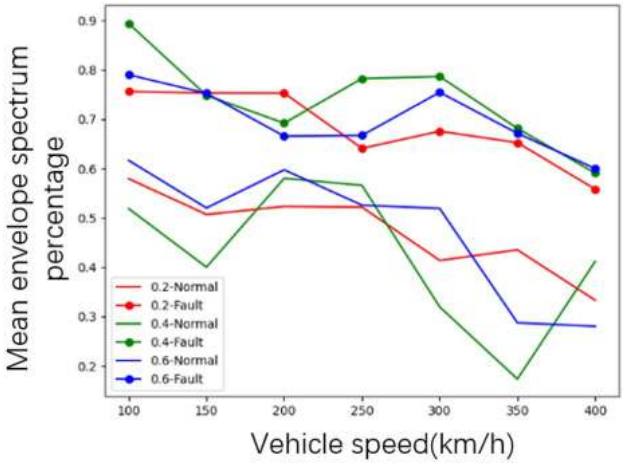


**Figure 15** Mean envelope spectrum percentage under different vehicle speeds and wheel flat depth

5. Average acceleration $\overline{a}$

The data obtained from the experimental simulation records the axle box acceleration, which is the average acceleration $\overline{a}$ . The definition is as follows (see Formulas 10):

$$\overline{a} = \frac{\sum_{i=0}^{n} a_i}{n} \tag{10}$$

Definition of mean acceleration of 'Fault' data (see Formulas 11):

$$\overline{a}_F = \frac{\sum_{i=0}^{n} a_{Fi}}{n} \tag{11}$$

Definition of mean acceleration of 'Normal' data (see Formulas 12):

$$\overline{a}_N = \frac{\sum_{i=0}^{n} a_{Ni}}{n} \tag{12}$$

The reason for adding the average acceleration as an annotation is to better describe the wheel flat's characteristics under the influence of multiple factors.

6. Wheel flat depth $\boldsymbol{d}$

According to the fusion data obtained from the experimental simulation, the depth of the wheel flat is $d = 0.2mm$, $d = 0.4mm$, and $d = 0.6mm$ respectively. The 'Normal' data can be considered as no wheel flat, that is, the depth of the flat scar is d=0mm. For the above four cases, $d = 0mm$, $d = 0.2mm$, $d = 0.4mm$, and $d = 0.6mm$ are marked as 0, 1, 2, and 3.

### 3.3 Data batch

After the introduction of the processing of single experimental simulation data in Section 3.1 and Section 3.2, in this section, we will introduce how to complete the batch processing and marking of experimental simulation data to label and build the experimental detection data set by an automatic whole-process algorithm (see Figure 16). First, we traversed the experimental data file, obtain the file name to get the wheel flat depth, and vehicle speed, and read the time and acceleration data. Then since the sampling frequency and time segment are known, we calculated the number of slices. Finally, we finished slicing the periodic data and then slice the periodic data into 'Normal' and 'Fault' data to complete the data annotation.

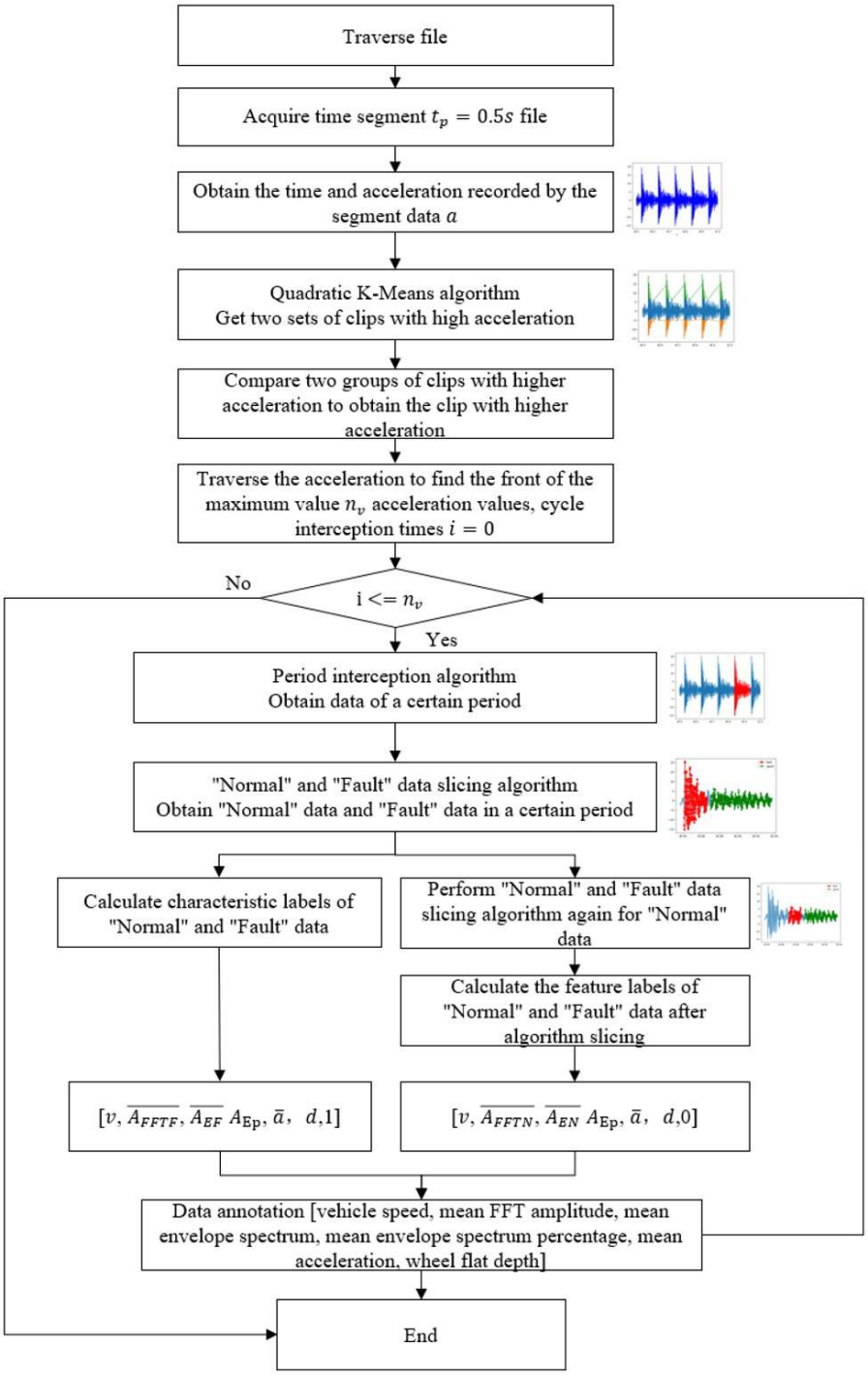


**Figure 16** An automatic whole-process algorithm for labeling the experimental detection data set

## 4 DETECTION MODEL

In this section, we constructed the wheel flat detection model with the data set constructed in section 3 and the machine learning model based on logistic regression and the K-nearest neighbor algorithm at first. Then to find the optimal model, we analyzed the effect of different labels on the accuracy of the detection model. Finally, we verified the data fusion to improve the detection accuracy of the detection model.

### 4.1 Model construction

The core of the detection model constructed in this paper is that data processing assists machine learning models to build data-driven intelligent detection models. The detection model we proposed needs to solve two tasks, one is to detect whether the wheel flat exists while the second is to answer the wheel flat depth in the presence of the wheel flat.

Therefore, we can understand the two tasks as a binary classification task and a multi-classification task. For different tasks, we constructed different detection models.

Logistic regression is to measure the relationship between the dependent variable and one or more independent variables, which is often applied to solve a binary classification task. Therefore, we choose to use it to solve the problem of detecting the existence of the wheel flat. The machine learning models based on solving multi-classification include Naive Bayes, Decision Tree, Random Forest, and so on. Through the comparison results of pre-experiments, we choose the machine learning model based on the K-nearest neighbor to solve the problem of identifying the depth of the wheel flat based on the comprehensive consideration of the time cost of recognition and the accuracy of recognition.

### 4.2 Model optimal

We focus on the impact of data annotation on the detection and recognition of scratches in this section. The purpose is to find the optimal detection model, that is, the least number of labels with a machine learning model to complete the detection and recognition. The analysis sample of the experiment is as follows: The total number of samples is 32040, of which the training set size is 2242, and the test set size is 9612.

We analyzed different angle which is on the time domain, frequency domain, and time-frequency domain. In each analysis, we used the logistic regression algorithm to detect whether the vehicle has a wheel flat and the K-nearest neighbor algorithm to identify the wheel flat depth. The results are as follows:

In the time domain analysis, we try to use the mean acceleration and vehicle speed to characterize the features of the wheel flat. The detection results are shown in Table 7:

**Table 7** The accuracy and recall rate of detection model.

| Method | Accuracy | Recall |
|---|---|---|
| Logistic regression | 74.8% | 69.4% |
| KNN | 89.9% | 88.5% |

The accuracy and recall rate of the detection model shows that it is the same as the pre-test results for a single sample. Based on human visual experience, it is impossible to distinguish whether the wheel flat exists and the wheel flat depth. Therefore, time domain analysis cannot achieve vehicle wheel flat detection well.

In the frequency domain analysis, we use the combination of the vehicle speed and mean FFT amplitude, mean envelope spectrum, and mean envelope spectrum percentage respectively to characterize the features of the wheel flat. The detection results are shown in Table 8:

**Table 8** The accuracy and recall rate of detection model.

| Label | Method | Accuracy | Recall |
|---|---|---|---|
| Mean FFT amplitude $\overline{A_{FFT}}$ | Logistic regression | 94.2% | 92.5% |
| | KNN | 90.3% | 87.5% |
| Mean envelope spectrum $\overline{A_E}$ | Logistic regression | 94.1% | 91.9% |
| | KNN | 86.2% | 81.2% |
| Mean envelope spectrum percentage $A_{\mathrm{Ep}}$ | Logistic regression | **94.3%** | **95.8%** |
| | KNN | 76.2% | 67.1% |

Based on the results of frequency domain analysis, The accuracy and recall rate of the identification model on the wheel flat depth is not good. Therefore, we introduce the time-frequency domain analysis which is a combination of vehicle speed and average acceleration and mean FFT amplitude, mean envelope spectrum, and mean envelope spectrum percentage respectively to characterize the features of the wheel flat. The detection results are shown in Table 9:

**Table 9** The accuracy and recall rate of detection model.

| Label | | Method | Accuracy | Recall |
|---|---|---|---|---|
| Average acceleration $\overline{a}$ | Mean FFT amplitude $\overline{A_{FFT}}$ | Logistic regression | **99.33%** | **99.36%** |
| | | KNN | 98.6% | 98.0% |
| | | Logistic regression | 97.4% | 96.3% |

| | | | |
|---|---|---|---|
| Mean envelope spectrum $\overline{A_E}$ | KNN | 97.7% | 96.8% |
| Mean envelope spectrum | Logistic regression | 95.4% | 96.0% |
| percentage $A_{\mathrm{Ep}}$ | KNN | 97.6% | 97.0% |

To sum up, for the detection results of time domain, frequency domain analysis, and time-frequency domain analysis, the conclusions are as follows:

1. The accuracy and recall rate of time-frequency domain analysis is higher than that of time-domain or frequency domain analysis.
2. In the frequency domain analysis, the detection model of whether wheel flat exists based on the logistic regression, the mean envelope spectrum percentage and vehicle speed used to train the model make the excellent performance on the accuracy and recall rate.
3. In the time-frequency domain analysis, identifying the wheel flat with labels on mean FFT amplitude, average acceleration and vehicle speed makes model have the excellent performance on the accuracy and recall rate.

### 4.3 Model evaluation

After finding the optimal detection model in section 4.2, we used the mean envelope spectrum percentage and logistic regression to build the detection model answering whether the wheel flat exists. While in response to the wheel flat depth, we use average acceleration and mean FFT amplitude to match the K-nearest neighbor to construct the identification model. We try to verify the idea that data fusion mentioned in Section 2 improves the improving detection accuracy. Combined with the influence of Vehicle-track rigid-flexible coupling dynamics simulation data (SIMPACK simulation data) and data obtained from wheel flats fault simulation based on rolling test bench experiment (real test data) on the accuracy of the detection model, we designed the following experiments as follow:

The training sets are SIMPACK simulation data, real test data, and SIMPACK simulation data and real test data separately, and the machine learning models are logistic regression and K-nearest neighbor. We use mean square error (MSE) and R-square to measure the quality of the model. Among them, the mean square error is used to evaluate the degree of change in the data. The smaller the value of MSE, the better the accuracy of the prediction model to describe the experimental data. The R-square is to characterize the quality of a fit through the change of the data. The closer to 1, the better the model fits the data. The experimental results are shown in Table 10, which shows that the detection model trained with SIMPACK simulation data and real test data performs well in detection accuracy. Therefore, we finished one of the purposes this paper proposed which is to reduce detection costs and improve detection accuracy.

**Table 10** Evaluation results of detection model under data fusion.

| Testing sets | Detection model | | Mean-square error (MSE) | R-square |
|---|---|---|---|---|
| | Training sets | machine learning model | | |
| Simpack+ Real test | Simpack | Logistic regression | 0.3366 | -0.353 |
| | | K-nearest neighbor | 0.297 | -0.189 |
| | Real test | Logistic regression | 0.069 | 0.72 |
| | | L-nearest neighbor | 0.148 | 0.401 |
| | Simpack+ Real test | Logistic regression | 0.003 | 0.987 |
| | | Logistic regression | 0.002 | 0.989 |

## 5 CONCLUSION

To solve the problem of large amounts of data processing, reduce the detection cost as much as possible, and improve the detection accuracy, this paper constructs an intelligent whole-process data processing method and a detection wheel flat model. Based on the idea of data fusion, we combined vehicle-track rigid-flexible coupling dynamics simulation data with data obtained from wheel flats fault simulation based on a rolling test bench experiment to construct the detection model to reduce the detection cost. At the same time, this paper focuses on an intelligent whole-process data processing method of wheel flat fault feature extraction and labeling to solve large amounts of data processing. Through the constructed experimental detection data set, the machine learning model is used to construct the recognition and detection model of the vehicle wheel flat.

The innovations and contributions of this paper are as follows:

First, we combined vehicle-track rigid-flexible coupling dynamics simulation data with data obtained from wheel flats fault simulation based on a rolling test bench experiment based on the idea of data fusion to construct the detection model to reduce the detection cost and improve the detection accuracy.

Secondly, we proposed an automatic whole-process algorithm for labeling the experimental detection data set. In the extraction of data feature fragments, we proposed the method of secondary K-Means to realize the automatic extraction of slice data and the automatic extraction of data containing the fault and normal signals in periodic data.

The third is to propose a physical quantity that characterizes the features of the wheel flat which is the mean envelope spectrum percentage. We used mean envelope spectrum percentage to train the model based on the logistic regression, which makes the excellent performance on the accuracy and recall rate of detecting whether wheel flat exists. The accuracy is 94.3 %.

Finally, we constructed the intelligent detection model by using the constructed experimental detection data set to assist the machine learning model to complete the identification and detection of vehicle wheels flat. Through the analogy experiment, it is found that combined average acceleration with Mean FFT amplitude to train the model based on the K-nearest neighbor, which the detection model makes the excellent performance on the accuracy and recall rate of identifying the wheel flat depth. The accuracy is 98.6 %.

The contribution of this paper is mainly reflected in the application of computer science in the field of fault identification of railway transportation, further in promoting the automation and intelligence of the traditional machinery industry, and in providing research ideas for the development of massive data analysis and health management system.

## Acknowledgements

This research is based upon work supported by China Academy of Railway Sciences Fund Project (contract No.2022YJ145), Beijing Natural Science Foundation and Fengtai Rail Transit Frontier Research Joint Fund L191009, the National Natural Science Foundation of China (No. 61877002), and scientific research program of Beijing Municipal Education Commission KZ202110011017.

**Author's Contribuitions:** Conceptualization, Xiang Su and Nan Li; Methodology, Xiang Su; Investigation, Xiang Su, Guangwei Zhao and Yuxin Sun; Writing - original draft, Xiang Su, Guangwei Zhao and Yuxin Sun; Writing - review & editing, Xiang Su; Funding acquisition, Guangwei Zhao and Nan Li; Resources, Guangwei Zhao and Nan Li; Supervision, Xiang Su.

**Editor:** Rogério José Marczak

## References

Xing, ZY., Zhang ZY., Yao XW., Qin Y., Jia LM, (2022). Rail wheel tread defect detection using improved YOLOv3, MEASUREMENT 203:111959.

Bernal, E., Spiryagin, M., Cole, C, (2022). Wheel flat detectability for Y25 railway freight wagon using vehicle component acceleration signals. VEHICLE SYSTEM DYNAMICS 58(12):1893-1913.

Trilla, A., Bob-Manuel, J., Lamoureux, B., Vilasis-Cardona, X, (2021). Integrated Multiple-Defect Detection and Evaluation of Rail Wheel Tread Images using Convolutional Neural Networks. INTERNATIONAL JOURNAL OF PROGNOSTICS AND HEALTH MANAGEMENT 12(1):1-19.

Liu XZ, Ni YQ, (2018). Wheel tread defect detection for high-speed trains using FBG-based online monitoring techniques. SMART STRUCTURES AND SYSTEMS 21(5):687-694.

Cao WJ., Zhang SL., Bertola NJ., Smith IFC., Koh CG, (2019). Time series data interpretation for 'wheel-flat' identification including uncertainties. STRUCTURAL HEALTH MONITORING-AN INTERNATIONAL JOURNAL 22(1):3-18.

Li CS., Luo SH., Cole C, Spiryagin M, (2017a). An overview: modern techniques for railway vehicle on-board health monitoring systems. VEHICLE SYSTEM DYNAMICS 55(7):1045-1070.

Gao, R., He, QX, Feng, QB. (2019). Railway Wheel Flat Detection System Based on a Parallelogram Mechanism. SENSORS 19(16): pp.1-13.

Bernal E., Spiryagin M., Cole C, (2021). Wheel flat analogue fault detector verification study under dynamic testing conditions using a scaled bogie test rig. INTERNATIONAL JOURNAL OF RAIL TRANSPORTATION 10:177-194.

Komorski, P., Szymanski, GM., Nowakowski, T., Orczyk, M, (2021). Advanced acoustic signal analysis used for wheel-flat detection. LATIN AMERICAN JOURNAL OF SOLIDS AND STRUCTURES 18(1):1-14.

Zhou QB., Chen RW., Huang B., Liu C., Yu J., Yu XQ, (2019). An Automatic Surface Defect Inspection System for Automobiles Using Machine Vision Methods. SENSORS 19(3):644-662.

Xu JY., Sun R., Tian YP., Xie Q., Yang Y., Liu HD., Cao L, (2015). Correction of rolling wheel images captured by a linear array camera. Applied Optics 54(33):9736-9740.

BERNAL, E J., MARTINOD, R M., BETANCUR G R, (2016). Partial-profilogram reconstruction method to measure the geometric parameters of wheels in dynamic condition. VEHICLE SYSTEM DYNAMICS 54(5):606-616.

Alireza Alemi., Francesco Corman., Gabriel Lodewijks, (2017). Condition monitoring approaches for the detection of railway wheel defects. The Journal of Rail and Rapid Transit 231(8):961-981.

Xiao Q., Jiang XF., Liu HT., Xie FY., Zhou ST, (2021). Research on Real-Time Monitoring Methods for Railroad Wheel Tread Defects: A Review. Journal of East China Jiaotong University 38(4):99-112.

Yi C., Huo HX., Liao XK., Zhou L., Ran L., Lin JH, (2022). Investigation on the characterisation of axle box resonance characteristics to wheel excitation. VEHICLE SYSTEM DYNAMICS. DOI: 10.1080/00423114.2022.2103437

Li YF., Zuo MJ., Lin JH., Liu JX, (2017b). Fault detection method for railway wheel flat using an adaptive multiscale morphological filter. Mechanical Systems and Signal Processing 84:642-658.

Song Y., Zhang XM., Sun B, (2021). Influence of Polygonal Wear on Dynamic Performance of Wheels on High-Speed Trains. TEHNICKI VJESNIK-TECHNICAL GAZETTE 28(1):27-33.

Mohammadi M, Mosleh A, Vale C, Ribeiro D, Montenegro P, Meixedo A, (2023). An Unsupervised Learning Approach for Wayside Train Wheel Flat Detection. SENSORS 23(4):1-27.

Shim, J., Koo J., Park Y., Kim J, (2022). Anomaly Detection Method in Railway Using Signal Processing and Deep Learning. Applied Sciences 12:12901.